

# PHYSICAL REVIEW C

## NUCLEAR PHYSICS

THIRD SERIES, VOLUME 44, NUMBER 6

DECEMBER 1991

### RAPID COMMUNICATIONS

*The Rapid Communications section is intended for the accelerated publication of important new results. Manuscripts submitted to this section are given priority in handling in the editorial office and in production. A Rapid Communication in Physical Review C may be no longer than five printed pages and must be accompanied by an abstract. Page proofs are sent to authors.*

#### Energy partition in near-barrier strongly damped collisions $^{58}\text{Ni} + ^{208}\text{Pb}$

M. B. Chatterjee, S. P. Baldwin, J. R. Huizenga, D. Pade,\* B. M. Quednau, W. U. Schröder,  
B. M. Szabo, and J. Töke

*Department of Chemistry and Nuclear Structure Research Laboratory, University of Rochester, Rochester, New York 14627*  
(Received 26 July 1991)

Neutron spectra from the inverse-kinematics reaction  $^{58}\text{Ni} + ^{208}\text{Pb}$  at  $E_{\text{lab}}/A = 6.65$  MeV have been measured in coincidence with nickel-like fragments. Neutron emission patterns for net pickup and stripping channels have been analyzed in terms of sequential evaporation from fully accelerated projectilelike and targetlike fragments. As at higher energies, these patterns suggest an absence of appreciable correlations between net mass transfer and excitation energy division for strongly damped collisions, at the present near-barrier energy. The overall multiplicities, as well as energy spectra and angular distributions of neutrons, are well reproduced by simulation calculations, assuming an energy division always in favor of the heavy fragment.

In recent years, considerable effort has been focused on determining how the heat generated in the process of energy dissipation is divided between the two fragments from a damped reaction at a few MeV per nucleon above the barrier [1–10]. It has been established that at low kinetic-energy losses, the two fragments receive approximately equal excitation energies, when averaged over mass asymmetry, while at large energy losses, this excitation energy division approaches the limit corresponding to equal fragment temperatures [1–5]. Such trends are quite well understood within the framework of the nucleon exchange model [11], although a fully quantitative description has not been achieved as yet. In a number of more recent studies [6–10], correlations between excitation energy division and net mass transfer were investigated. In some of these studies, conclusions were reached that are difficult to reconcile with the stochastic nucleon exchange (NEM) picture of the interaction. It has been reported [6–8] that, at any fixed total kinetic-energy loss, disproportionately large fractions of the total excitation energy are found in the net acceptor fragments. As a consequence of these reports, alternative reaction models have been proposed [12–14] for an explanation of the effect.

Subsequent reexamination [15–17] of some of the experimental data obtained in the kinematical coincidence

experiments [6–8] at a few MeV per nucleon above the barrier has shown that the reported correlations result to a large extent from deficiencies in the data analysis procedure employed. However, results of radio-chemical studies [10,11] of asymmetric reaction systems at near-barrier energies continue to present a challenge to the current understanding of the reaction dynamics. Although it seems quite possible that the reaction mechanism changes significantly at near-barrier energies, one realizes that the conclusions of the above studies rely crucially on unproven assumptions on the time scale of charge density equilibration in damped reactions. The present experimental study of the reaction  $^{58}\text{Ni} + ^{208}\text{Pb}$  at a c.m. energy of about 80 MeV above the barrier was undertaken, in order to obtain independent and more direct evidence on the magnitude of the correlations between mass transfer and energy division at near-barrier energies.

The exclusive experiment measuring neutrons in coincidence with reaction fragments was carried out at the Super HILAC facility of the Lawrence Berkeley Laboratory. A 1.5-mg/cm<sup>2</sup>-thick  $^{58}\text{Ni}$  target was bombarded with a  $^{208}\text{Pb}$  beam of  $E_{\text{lab}}/A = 6.65$  MeV. The reaction channels of interest, i.e., those corresponding to net pickup or net stripping by the projectile, were identified by measuring the nickel-like [targetlike fragment (TLF)] recoiling fragments with an array of silicon detector tele-

scopes. Some of these telescopes were operated in  $\Delta E$ - $E$  time-of-flight mode, and provided information on the fragment masses, in addition to an identification according to their atomic numbers  $Z$ . Data discussed here were obtained mainly with one of the telescopes, placed at an angle of  $-35^\circ$  and at a distance of approximately 12 cm from the target, operated in the simpler  $\Delta E$ - $E$  mode. This angle is somewhat smaller than the laboratory grazing angle of the measured Ni-like (TLF) fragments of  $\theta_g = 48^\circ$ . The data obtained with the telescope were used to identify, in an iterative fashion, the binary reaction channel and to reconstruct the preevaporation kinematics, i.e., the fragment velocity vectors, kinetic-energy loss ( $E_{\text{loss}}$ ), the center-of-mass angles, etc. In addition, the  $\Delta E$  detector of this telescope also provided the start signal for the time-of-flight (TOF) measurement of the associated neutrons.

Neutrons were measured with nine detectors placed in plane with the telescope at angles ( $\theta_{\text{lab}}$ ) between  $-65^\circ$  and  $+100^\circ$  at distances from the target ranging from 80 to 120 cm. The detectors consisted of cylindrical NE213 liquid-scintillator cells 12.7 cm in diameter and 2.5–5.0 cm in length viewed by AMPEREX XP2041 photomultipliers.

Experimental results are shown in Figs. 1–4, together with the results of the corresponding simulation calculations. The coincidence data in these figures were sorted into five bins in TLF atomic numbers and two bins in energy loss. In Figs. 1 and 2, neutron spectra  $d^2m/(dEd\Omega)_{\text{lab}}$  are exhibited for the two angles  $\theta = 12^\circ$  and

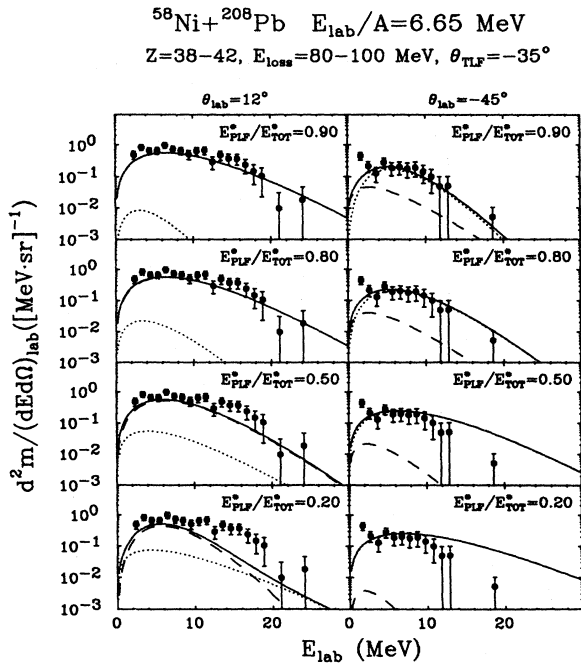


FIG. 1. Neutron energy spectra from the  $^{58}\text{Ni} + ^{208}\text{Pb}$  reaction at  $E_{\text{lab}}/A = 6.65$  MeV measured at  $12^\circ$  and  $-45^\circ$  in coincidence with TLF's with  $Z = 38$ – $42$ , corresponding to stripping by the projectile. Solid dots represent experimental data. Solid lines denote total yields, while dashed and dotted lines depict contributions from the two sources considered, PLF's and TLF's, respectively.

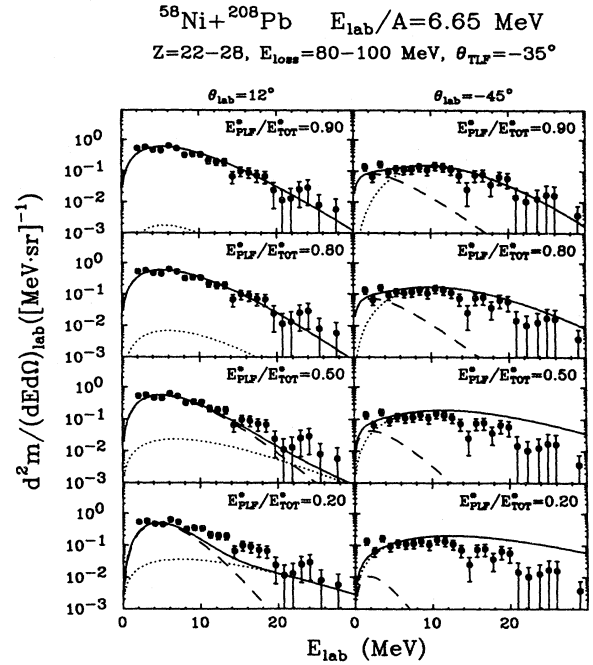


FIG. 2. Neutron energy spectra from the  $^{58}\text{Ni} + ^{208}\text{Pb}$  reaction at  $E_{\text{lab}}/A = 6.65$  MeV measured at  $12^\circ$  and  $-45^\circ$  in coincidence with TLF's with  $Z = 22$ – $28$ , corresponding to pickup by the projectile. Solid dots represent experimental data. Solid lines denote total yields, while dashed and dotted lines depict contributions from the two sources considered, PLF's and TLF's, respectively.

$-45^\circ$ , where  $m$  is the neutron multiplicity. These angles are close to the reaction angles of projectilelike fragments (PLF) and TLF, respectively, as selected by the trigger telescope at  $\theta = -35^\circ$ . Figures 1 and 2 correspond to net stripping and pickup of mass, respectively, by the projectile, and fully damped ( $E_{\text{loss}} = 80$ – $100$  MeV) collisions.

In these figures, the data points are compared on a logarithmic scale to results of model calculations (curves) assuming sequential neutron emission from the fully accelerated primary PLF and TLF. In these calculations, as well as in the reconstruction of the event kinematics based on the PLF atomic number and energy, it was assumed that the primary masses of the PLF and TLF,  $A_{\text{PLF}}$  and  $A_{\text{TLF}}$ , respectively, are proportional to their atomic numbers, such that, e.g.,  $A_{\text{PLF}} = Z_{\text{PLF}}^* A_{\text{tot}} / Z_{\text{tot}}$ . It was further assumed that the (neutron-rich) fragments evaporate neutrons isotropically, as long as their excitation energy exceeds the neutron binding energy, and that the neutron energy spectra are Maxwellian, with a slope parameter of  $T = (8E^*/A)^{1/2}$ . The effect of the uncertainty of such assumptions on the obtained results is negligible, as compared to the overall rather large uncertainty of the extracted value of  $E_{\text{PLF}}^*/E_{\text{tot}}^*$ . It is worth pointing out that, unlike the methods that fully rely on the accuracy of the measurement of the fragment mass, such as, e.g., the kinematical coincidence or radio-chemical methods, the present method of determining the excitation energy division from the observed neutron emission patterns does not require an accurate knowledge of the fragment

masses. Uncertainties in fragment masses affect the results of the latter method only in higher order, e.g., through the reconstructed velocity vectors, kinetic-energy loss, and the neutron binding energy. Furthermore, the quality of the achieved fit to the observed emission patterns provides for an independent test of all assumptions made in the simulation calculations. Various divisions of the total excitation energy  $E_{\text{tot}}^*$  were considered, as indicated in the individual panels by the corresponding ratios  $E_{\text{PLF}}^*/E_{\text{tot}}^*$ . Such a two-source model is expected to be sufficient, because additional components of neutrons such as emitted in a preequilibrium cascade or during the acceleration phase are expected to be weak at the low bombarding energy studied here. The contributions of PLF and TLF to the total yield (solid curves) are illustrated by the dashed and dotted curves, respectively. Already, from a cursory inspection of the data displayed in Figs. 1 and 2, one concludes that the relative yields of PLF and TLF neutrons do not depend strongly on the direction of mass flow between the reaction partners. Figure 1 corresponds to stripping of 10–14 protons off the projectile (pickup by the target), i.e., a loss of 20–28 nucleons by the Pb-like fragment. Yet, as seen from the comparison between data and the solid theoretical curves, the heavy Pb-like donor nucleus acquires significantly more than 50%, and perhaps as much as 80%–90% of the total amount of excitation energy generated in the collision. Conversely, the target acquires a relatively small fraction of the total excitation energy, even though it has picked up the same number of nucleons. As illustrated by the spectra displayed in the lower half of Fig. 1, the opposite assumption, corresponding to a division of the excitation energy in favor of the TLF ( $E_{\text{PLF}}^*/E_{\text{tot}}^* \geq 50\%$ ), leads to an underestimation of the experimental spectrum at  $\theta = 12^\circ$  by a significant factor, while the experimental spectrum at  $\theta = -45^\circ$  is

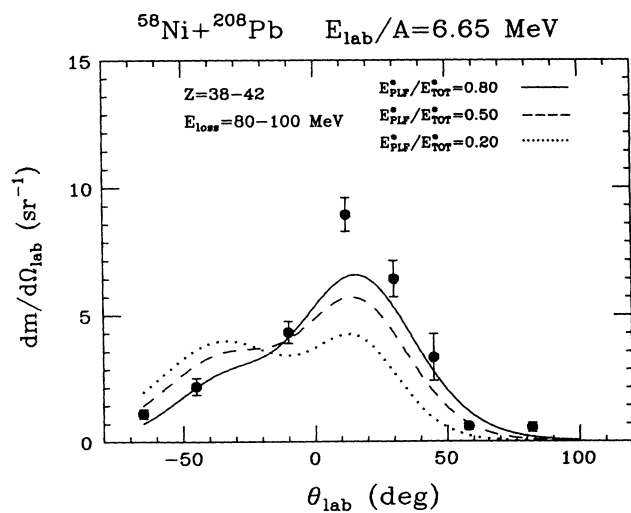


FIG. 3. Angular distribution of neutrons from the  $^{58}\text{Ni} + ^{208}\text{Pb}$  reaction at  $E_{\text{lab}}/A = 6.65$  MeV in coincidence with TLF's with  $Z = 38-42$ . Solid dots represent experimental data, while solid, dashed, and dotted curves are results of simulation calculations assuming three different excitation energy divisions as indicated in the upper right corner.

overestimated. Similar amounts of excitation energy are deposited in the Pb-like fragment, when it picks up mass from the TLF, as seen from Fig. 2. This energy division is close to that corresponding to thermal equilibrium, where fragments acquire excitation energies approximately in proportion to their masses. For this second bin in the atomic number of the TLF,  $22 \leq Z_{\text{TLF}} \leq 28$ , unlike for the first bin, there is an appreciable probability for the PLF to undergo fission. For the highest excitation energy of 81 MeV of the PLF considered, this probability ranges from approximately 1.5% ( $Z_{\text{PLF}} = 82$ ) to 57% for the highest atomic number of  $Z_{\text{PLF}} = 88$ . When weighted with the distribution of the atomic numbers within the  $Z$  bin considered, this probability is approximately 17%. Because of the relatively high velocity of the PLF, the secondary fission of the PLF at such a rate and the subsequent emission of neutrons from the fission fragments has a negligible effect on the theoretical curves in Figs. 2 and 4. It is worth pointing out that, because of kinematical focusing of neutrons, even an assumption of a 100% probability for PLF fission will not change the theoretical curves dramatically. However, it would lead to an even higher value of the extracted ratio of  $E_{\text{PLF}}^*/E_{\text{tot}}^*$ , with a poorer overall quality of the fit.

While Figs. 1 and 2 refer to only two neutron detection

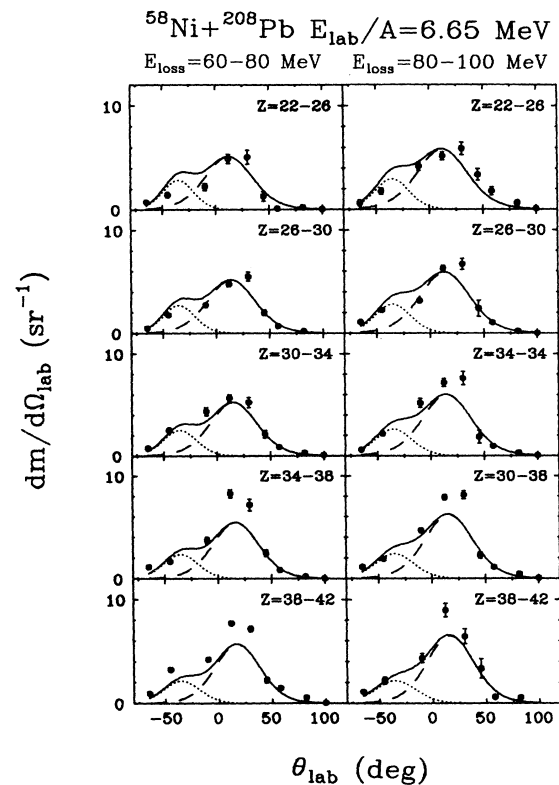


FIG. 4. Angular distribution of neutrons from the  $^{58}\text{Ni} + ^{208}\text{Pb}$  reaction at  $E_{\text{lab}}/A = 6.65$  MeV in coincidence with TLF's. Solid dots represent experimental data, while solid, dashed, and dotted curves are results of simulation calculations for the total neutron yield and the contributions from PLF's and TLF's, respectively, assuming  $E_{\text{PLF}}^*/E_{\text{tot}}^* = 0.8$ .

angles, the angular distributions  $dm/d\Omega_{\text{lab}}$  sampled with all detectors are displayed in Figs. 3 and 4, for different bins in kinetic-energy loss and TLF atomic number  $Z$ . The modest but adequate sensitivity of the angular distribution of the multiplicity to the excitation energy division is illustrated in Fig. 3. Here, the data points for  $E_{\text{loss}} = 80\text{--}100$  MeV and substantial net mass transfer to the TLF are compared to theoretical angular distributions (curves) calculated for various assumed divisions of the total energy loss between the fragments. As seen from the comparison in Fig. 3, the best overall reproduction of the data is achieved with the assumption (solid curve) that 80% of the dissipated energy is deposited in the Pb-like fragment, which is the donor in this case. The same assumption about the excitation energy division provides a satisfactory description of the angular distributions, for the entire range of charge asymmetries and energy losses, measured with sufficient accuracy in the present work. This is evident from the angular distributions of neutrons shown in Fig. 4 for five successive bins in TLF atomic number, for each of the two different  $E_{\text{loss}}$  bins. In this

figure, the components of neutrons from the TLF and PLF are depicted as dotted and dashed curves, respectively, while the total yields are represented by solid lines.

In summary, it has been found for the strongly damped reaction  $^{58}\text{Ni} + ^{208}\text{Pb}$  at the near-barrier energy of  $E_{\text{lab}}/A = 6.65$  MeV that the sharing of the dissipated energy between the reaction partners is not influenced appreciably by magnitude and direction of the net charge (and mass) transfer. These findings are at variance with observations reported [9,10] for similar systems at only slightly lower bombarding energies. On the other hand, the results of the present work are consistent with the trends established at higher bombarding energies. These results are also compatible with the current understanding of the low-energy reaction dynamics in terms of the nucleon exchange model [11].

This work was supported by the U.S. Department of Energy, Grant No. DE-FG02-88ER40414. The authors would like to thank Dr. R. T. deSouza for his assistance with the experiment.

\*Now at Dornier GmbH, Unteruerdingen, Germany.

- [1] T. C. Awes, R. L. Ferguson, R. Novotny, F. E. Obenshain, F. Plasil, S. Pontoppidan, V. Rauch, G. R. Young, and H. Sann, *Phys. Rev. Lett.* **52**, 251 (1984).
- [2] R. Vandenbosch, A. Lazzarini, D. Leach, D. K. Lock, A. Ray, and A. Seamster, *Phys. Rev. Lett.* **52**, 1964 (1984).
- [3] H. Sohlbach, H. Freiesleben, W. F. W. Schneider, P. Braun-Munzinger, D. Schüll, B. Kohlmeyer, M. Marinescu, and F. Pühlhofer, *Phys. Lett.* **153B**, 386 (1985); H. Sohlbach, H. Freiesleben, W. F. W. Schneider, D. Schüll, P. Braun-Munzinger, B. Kohlmeyer, M. Marinescu, and F. Pühlhofer, *Nucl. Phys. A* **467**, 349 (1987); H. Sohlbach, H. Freiesleben, W. F. W. Schneider, D. Schüll, B. Kohlmeyer, M. Marinescu, and F. Pühlhofer, *Z. Phys. A* **328**, 205 (1987).
- [4] L. G. Sobotka, G. H. Wozniak, R. J. McDonald, M. A. McMahan, R. J. Charity, L. G. Moretto, Z. H. Liu, F. S. Stephens, R. M. Diamond, and M. A. Deleplanque, *Phys. Lett. B* **175**, 27 (1986).
- [5] J. L. Wile, W. U. Schröder, J. R. Huizenga, and D. Hilscher, *Phys. Rev. C* **35**, 1608 (1987).
- [6] D. R. Benton, H. Breuer, F. Khazaie, K. Kwiatkowski, V. E. Viola, A. C. Mignerey, and A. P. Weston-Dawkes, *Phys. Rev. C* **38**, 1207 (1988).
- [7] R. Płaneta, K. Kwiatkowski, S. H. Zhou, V. E. Viola, H. Breuer, M. A. McMahan, J. Randrup, and A. C. Mignerey, *Phys. Rev. C* **39**, 1197 (1989).
- [8] K. Kwiatkowski, R. Płaneta, S. H. Zhou, V. E. Viola, H. Breuer, M. A. McMahan, and A. C. Mignerey, *Phys. Rev. C* **41**, 958 (1990).
- [9] H. Keller, R. Bellwied, K. Lützenkirchen, J. V. Kratz, W. Brüche, H. Gäggeler, K. J. Moody, M. Schädel, and G. Wirth, *Z. Phys. A* **328**, 255 (1987).
- [10] W. U. Scherer, W. Brüche, M. Brügger, C. Frink, H. Gäggeler, G. Herrmann, K. V. Kratz, K. J. Moody, M. Schädel, K. Sümmerer, N. Trautmann, and G. Wirth, *Z. Phys. A* **335**, 421 (1990).
- [11] J. Randrup, *Nucl. Phys. A* **327**, 490 (1979); **383**, 468 (1982).
- [12] A. Grossman and U. Brosa, *Nucl. Phys. A* **481**, 340 (1990).
- [13] J. Wilczyński and H. W. Wilshut, *Phys. Rev. C* **39**, 2475 (1989).
- [14] J. Wilczyński and K. Siwek-Wilczyńska, *Phys. Rev. C* **41**, R1917 (1990).
- [15] J. Töke, W. U. Schröder, and J. R. Huizenga, *Phys. Rev. C* **40**, R1577 (1989).
- [16] J. Töke, W. U. Schröder, and J. R. Huizenga, *Nucl. Instrum. Methods Phys. Res. Sect. A* **228**, 406 (1990).
- [17] J. Töke, R. Płaneta, W. U. Schröder, and J. R. Huizenga, *Phys. Rev. C* **44**, 390 (1991).